

ANALYSIS OF VAPOR CONDENSATION PROCESS FROM MOIST AIR

تحليل إجراء تكثيف البخار من هواء رطب

M. G. Wasel*, M. G. Mousa ** and Marzouk. A. Omer*

* Faculty of Engineering, Mansoura Univ., Mansoura, Egypt,

** Faculty of Education, Industrial Branch Damietta, Mansoura Univ., Mansoura, Egypt

Email: mgmoussa@hotmail.com

الخلاصة: تم في هذا البحث دراسة نظرية ومعملية لتكثيف بخار الماء من هواء رطب يمر على سطح أفقي بارد ولهذا أهمية في التطبيقات الهندسية وخصوصاً في معالجة الهواء الرطب. في الدراسة النظرية تم فرض أن السريان رقائقي مستقر وخواصه الفيزيائية ثابتة. باستخدام معادلات السريان والطاقة والتركيز وفرض متغيرات مستقلة وتابعة لا بعدية تم تحويل المعادلات الواسفة للسريان إلى معادلات تفاضلية عادية لا بعدية. تم حل هذه المعادلات عددياً بتطبيق طريقة رانج كوتا مصحوبة بطريقة الرصد. تم حساب توزيع السرعة ودرجة الحرارة والتركيز اللا بعدية وكذلك استنتاج علاقات بين أرقام نوسلت وشيروود كوال في رقم رينولدز عند قيم مختلفة لأرقام براننل وشميدت. في الدراسة المعملية تم دراسة سريان الهواء الرطب داخل نفق هوائي أبعاده (1200 × 300 × 200 مم) وسطحه السفلي مبرد بواسطة وحدة تبريد منفصلة. نتيجة لهذا التبريد فإن جزء من بخار الماء المحمل في الهواء يتم تكثفه على اللوح الأفقي البارد. تم إجراء التجارب عند قيم مختلفة لسرعة الهواء داخل النفق. أثناء هذه التجارب تم قياس درجة الحرارة الجافة والرطوبة عند مواضع مختلفة بطول وعرض وارتفاع النفق. أمكن الحصول على توزيع درجات الحرارة وتقدير كمية المياه المتكاثفة لكل تجربة ثم تم إيجاد علاقة بين أرقام نوسلت وشيروود لقيم مختلفة لسرعة الهواء الرطب (قيم مختلفة لرقم رينولدز) داخل النفق. لوحظ من هذه العلاقة أن أرقام نوسلت وشيروود تزيد إلى أكبر قيمة لها عند قيمة رينولدز 10×10^5 تقريباً وبزيادة رقم رينولدز تأخذ أرقام نوسلت وشيروود في التناقص وذلك بسبب نزوح قطرات من الماء مع الهواء المار على السطح البارد. تم مقارنة النتائج المعملية والنظرية ووجد أنها متوافقة بصورة مرضية. تم مقارنة النتائج المعملية بأخرى من أبحاث سابقة ووجد أنها متوافقة بصورة مرضية.

Keywords: Heat and Mass Transfer- Condensation- Moist Air

Abstract:

Condensation process, from moist airflow over flat plate, is investigated theoretically and experimentally. This process has many important engineering applications, which are concerning with moist air treatment.

In the theoretical analysis of the present work, the flow is assumed to be laminar, steady and of constant physical properties. The process is described by continuity, momentum, energy and concentration partial differential equations expressed in Cartesian coordinates system. Due to the nature of the studied problem and with proper transformation of the problem dependent and independent variables, these governing equations are transformed to set of ordinary differential equations. Accordingly, one can obtain similar solutions of the problem, which are obtained by application of the well-known numerical method Rung-Kutta accompanied with shooting method. According to this solution, the values of Nusselt and Sherwood numbers, for all values of Reynolds number are obtained.

The test section, of the experimental work, is a rectangular duct with cooled bottom. The moist air is forced to flow inside the duct, where some of water is condensed over its lower surface. The values of dry bulb temperature and wet bulb temperature are measured through out the flow field for different values of flow velocity. In accordance heat and mass transfer coefficients are estimated for different operating conditions. A correlation formula of the problem parameters is proposed.

According to the obtained experimental results, the average heat and mass transfer coefficients increases by increasing velocity up to certain value of it then decreases for more increase of velocity.

Comparisons are made between present obtained experimental results and those results obtained in previous work, exhibit good agreement in the studied region.

Nomenclature

Symbol	Definition	Units
A_s	Surface area of segment	m^2
A_c	Cross sectional area of test section	m^2
C_p	Specific heat	kJ/kg K
D	Mass diffusivity	m^2/s
f	Dimensionless stream function	----
h	Heat transfer coefficient	$\text{kW/m}^2 \cdot \text{K}$
hm	Mass transfer coefficient	m/s
h_{fg}	Latent heat of condensed water	kJ/kg
i	Specific enthalpy	kJ/kg
k	Thermal conductivity	kW/m K
L, H, W	Length, Height and Width of test section	mm
m''	Mass flux	$\text{kg}/(\text{m}^2 \text{ s})$
P	Pressure	Pa
q''	Heat flux	W/m^2
R	Dimensionless parameter $R = \frac{h_{fg}}{C_p \Delta T} \cdot \frac{\Delta \rho}{\rho}$	----
RH	Relative humidity	----
T	Temperature	K
u_∞	Velocity at edge of boundary layer	m/s
u	Velocity component in x-direction	m/s
v	Velocity component in y-direction	m/s
w	Humidity ratio	$\text{kg}_w/\text{kg}_{\text{dry air}}$
x, y, z	Cartesian coordinates	m
X, Y, Z	Dimensionless Cartesian coordinates $(x/L), (y/H), (z/W)$	----
Greek symbols:		
α	Thermal diffusivity $(k/\rho C_p)$	m^2/s
ϕ	Dimensionless concentration $(\rho - \rho_w)/(\rho_\infty - \rho_w)$	----
μ	Dynamic viscosity	N.s/m^2
η	Similarity independent variable	----
ν	Kinematics viscosity	m^2/s
θ	Dimensionless temperature $(T - T_w)/(T_\infty - T_w)$	----
ρ	Density	(kg/m^3)
ψ	Stream function	m^2/s
Subscript		
av	average	w wall L average
v	vapor	x local

1. Introduction and literature review:

Condensation heat transfer process is widely employed in heat exchange devices such as desalination units, refrigeration units, petroleum refinery and food industries. Although film condensation in a thin film over flat plate was studied theoretically and experimentally by number of workers [1-11], the condensation process seems to need more investigation for better understanding.

F. Legau Desesquelles et al [1 and 2], 1985 studied experimentally and numerically the dynamical behavior of laminar and turbulent boundary layers, inside which condensation

phenomena exists. Temperature difference between the cold wall and the saturated air- steam flow, at atmospheric pressure and moderate temperature, is not exceed 20°C .

A. Matuszkiewicz. et al [3], 1991 studied condensation heat transfer process in two-phase two components (air and water). An approximate analytical relation between the profiles of droplet mass fraction and temperature in the boundary layer was found. In the case of small temperature differences, the droplet mass fraction decreased for $Le < 1$ (Lewis number) and increases for $Le > 1$ as the temperature decreases in the condensation boundary layer.

M.A.Yaghoubi, et al [4], 1993 studied heat and mass transfer with dehumidification in laminar boundary layer flow along a cooled flat plate. The effects of dehumidification, from laminar flow humid air, over isothermal cooled flat plate had been investigated using the similarity principle.

Wel-mon Yan [5], 1995 studied, numerically, transport phenomena of developing laminar mixed convection heat and mass transfer in inclined rectangular ducts.

Y. Sun I. S. Gartshore. et al [6] 1995, studied, experimentally investigation of film cooling heat transfer using the mass / heat analogy. An experimental investigation has been carried out to determine the heat /mass transfer coefficient downstream of a two - dimensional, normal, film cooling injection slot. The plate downstream of the slot is porous and air contaminated with propane was bled through it. The propane concentration very close to the wall measured using a flame ionization detector mass transfer measurement The concentration was conducted for film cooling mass ratio ranging from 0.0 to 0.5.

Kuan-Tzong Lee [7], 1998 studied mixed convection heat transfer in horizontal rectangular ducts with wall transpiration effects. A detailed numerical study was carried out to examine the effects of wall transpiration on laminar mixed convection flow and heat transfer in the entrance region of horizontal rectangular ducts. The vorticity-velocity method was employed in the formulation of both thermal boundary condition of uniform heat flux and uniform wall temperature.

Hic Chan Kang. et al [8], 1999 studied characteristics of film condensation of supersaturated steam - air mixture on a flat plate. Experimental and numerical work were performed for laminar film condensation of steam-air mixture flow over a flat plate. For small temperature difference between the gas mixture at the cold wall, and gas mixture at the boundary layer, steam-air mixture can be treated as superheated gas.

A. G. Amr et al [9], 2001 studied effect of cold surface and ambient conditions on water extraction from atmospheric air. Effect of cold surface shape and surrounding air conditions were investigated experimentally, with free air motion for vertical plate, bare and finned tubes and with forced air motion for vertical plates. Test results showed that water extraction productivity per unit surface area increases with decrease of surface temperature, increase of surrounding air-dry bulb temperature and relative humidity.

In the present work, experimental and theoretical model of condensation is proposed, which lead to more accurate prediction of heat and mass transfer coefficients. In the theoretical model, the effect of mass transfer on the rate of heat transfer associated with condensation, of water vapor from moist air, is studied. The target of experimental study is to get relation for the heat and mass transfer coefficients over flat plate as functions of operating parameters.

2. Mathematical Model

In the following sections, the flow describing equations are listed, the carried out modifications and the used technique of solution are reported. In order to simplify the flow describing equations of condensation process from moist air flowing over horizontal flat plate, some assumptions are made. The condensation is assumed to take place at the free surface of condensation film. The flow is taken laminar and steady. Moreover, the physical properties of

moist air are assumed to be constant. According to the foregoing assumptions, the continuity, momentum, energy and mass transfer equations in Cartesian coordinates, see in figure (1), can be written as

$$\frac{\partial(\rho u)}{\partial x} + \frac{\partial(\rho v)}{\partial y} = 0 \quad (1)$$

$$u \frac{\partial u}{\partial x} + v \frac{\partial u}{\partial y} = \nu \frac{\partial^2 u}{\partial y^2} \quad (2)$$

$$u \frac{\partial T}{\partial x} + v \frac{\partial T}{\partial y} = \alpha \frac{\partial^2 T}{\partial y^2} + \frac{Dh_{fg}}{\rho C_p} \cdot \frac{\partial^2 \rho_v}{\partial y^2} \quad (3)$$

$$u \frac{\partial \rho_v}{\partial x} + v \frac{\partial \rho_v}{\partial y} = D \frac{\partial^2 \rho_v}{\partial y^2} \quad (4)$$

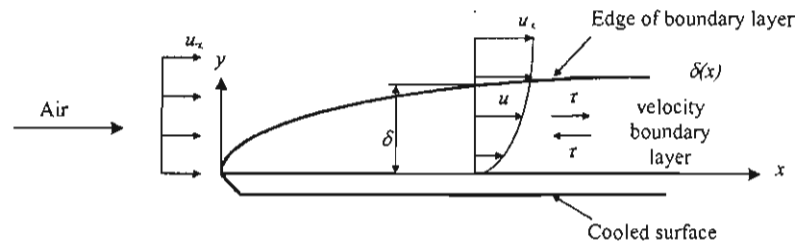


Figure (1) Schematic diagram of velocity boundary layer on a flat plate

Where u and v are the velocity components in x - and y -directions respectively. The temperature and the density are denoted by T and ρ . μ , α and D are the kinematic viscosity, thermal diffusivity and mass diffusivity respectively. Equations (1-4) must satisfy the following boundary conditions;

$$\begin{aligned} \text{At } y=0.0 & \quad u=0.0, \quad v=0.0, \quad T=T_w, \quad \rho=\rho_w \\ \text{At } y \rightarrow \infty & \quad u=u_\infty, \quad v=0.0, \quad T=T_\infty, \quad \rho=\rho_\infty \end{aligned} \quad (5)$$

Solving equations (1-4) with the boundary conditions (5), the velocity, temperature and density distributions through out the flow field can be obtained and consequently. Nusselt number and Sherwood number can be determined according to the following equations:

$$Nu_x = \frac{h \cdot x}{k}, \quad Sh_x = \frac{h_m \cdot x}{D} \quad (6)$$

Where h and h_m are heat and mass transfer coefficients.

Seeking for simplified form of flow governing equations (1-4), one introduces the following dimensionless form of dependent and independent variables of the problem:

$$\eta = y \sqrt{\frac{u_\infty}{\nu \cdot x}}, \quad \Psi = f(\eta), \quad \theta = \frac{T - T_w}{T_\infty - T_w} \quad \& \quad \phi = \frac{\rho_v - \rho_{v,w}}{\rho_{v,\infty} - \rho_{v,w}} \quad (7)$$

Where η , θ and ϕ are similarity variable, dimensionless stream function, dimensionless temperature and dimensionless concentration respectively. By substitution with equations (7) in equations (1-4), one can get the following dimensionless ordinary differential equations of flow describing equations:

$$f'''' + 0.5 f f'' = 0.0 \quad (8)$$

$$\theta'' + 0.5 Pr \cdot f \cdot \theta' = 0.0 \quad (9-a)$$

$$\theta'' + 0.5 Pr f \theta' - R Pr f \phi' = 0.0 \quad (9-b)$$

$$\phi'' + 0.5 Sc \cdot f \cdot \phi' = 0.0 \quad (10)$$

Where Pr and Sc are Prandtl and Schmidt numbers. R is a dimensionless number. They are defined through the following dimensionless numbers as;

$$Pr = \frac{\nu}{\alpha}, \quad Sc = \frac{\nu}{D}, \quad R = \frac{h_{fg}}{C_p \Delta T} \cdot \frac{\Delta \rho}{\rho}$$

Where ΔT is the temperature difference, $\Delta \rho$ is the density difference and h_{fg} is the latent heat of vaporization of water. Equations (9) are the energy equation in simpler form. As it is clear, equation (9-b) satisfies the case when interaction between heat and mass transfer processes is considered ($R \neq 0.0$).

The dimensionless form of boundary conditions of the flow describing equations (8-10) can be obtained with the aid of equations (5 and 7). Accordingly, these boundary conditions can be written as:

$$\text{At } \eta = 0.0, \theta = 0.0, \phi = 0.0 \quad \& \quad f' = 0.0 \quad (11)$$

$$\text{At } \eta \rightarrow \infty, \theta = 1.0, \phi = 1.0 \quad \& \quad f' = 1.0$$

Solving the above equations (8-11) the local Nusselt number and local Sherwood number as functions of dimensionless variables are obtained.

$$Nu_x / \sqrt{Re_x} = \left. \frac{\partial \theta}{\partial \eta} \right|_{\eta=0.0}, \quad Sh_x / \sqrt{Re_x} = \left. \frac{\partial \phi}{\partial \eta} \right|_{\eta=0.0} \quad (12)$$

Where Re_x local Reynolds number defined as;

$$Re = \frac{u_{\infty} \cdot x}{\nu}$$

Where x the length from the plate edge

2.1 Numerical Procedure

Since the derived flow governing equations (8-10) and their boundary condition (11) are ordinary differential equations of boundary value problem type, Rung-Kutta method is applied accompanied with shooting method to solve these equations. Computer Program is developed implementing the foregoing numerical technique in order to obtain the dimensionless velocity (f'), dimensionless temperature (θ) and dimensionless mass concentration (ϕ) throughout flow field ($\eta = 0.0$ to $\eta \rightarrow \infty$). Consequently, Nu_x and Sh_x are calculated.

3. Experimental Test Rig

In this section, a description of the experimental set-up is presented. The test rig is designed and constructed, such that one can investigate the effect of the operating parameters of condensation process above horizontal cooled flat plate. The details of test section, experimental and calculation procedure are presented below.

3.1 Description of test rig

The test section is designed and constructed, to study the parameters affecting the condensation process from moist air flowing in a horizontal rectangular duct with cooled bottom. The test section is attached to a wind tunnel, which uses atmospheric air at different

flow rates. Figure (2) shows the layout of the test rig including the designed test section. The

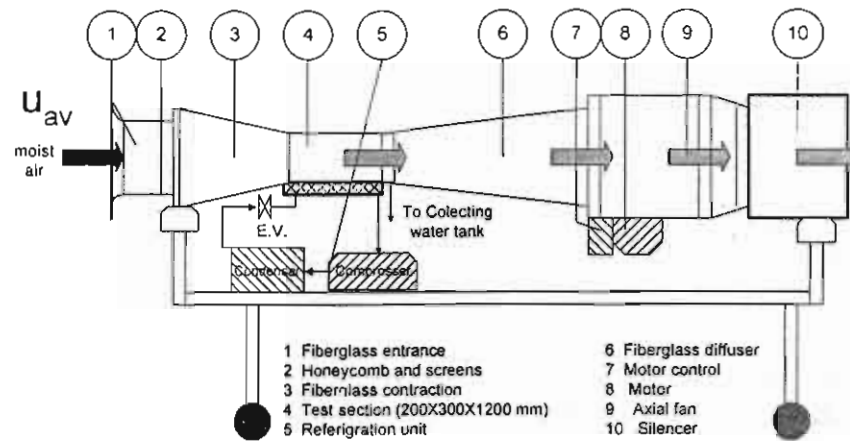


Figure (2) Wind tunnel

atmospheric moist air is drawn into the tunnel by axial fan (9), with varying flow rate from (0 to 22.5 m³/s) which is driven by a variable speed electric motor (8). In accordance, the mass flow rate of the tested air can be varied using the speed regulator (motor control) (7). The bottom of the test section is cooled using external refrigerating unit (5), which is driven by total input power to compressor 0.625 kW. Test section is a rectangular duct with dimensions (200×300×1200 mm) cooled bottom (3). A digital thermostat (4) is used to adjust the temperature of the cooled plate (3), by actuating or shutting down the compressor of the refrigeration unit. Test section is insulated by glass wool layer (6) in three sides while the fourth side (300×1200 mm) is made from PVC plate (2). Five, equally spaced rectangular slots with dimensions (12×300 mm) each, at $x = 0.0, 300, 600, \dots$ and 1200 mm are cut in front the PVC side, as shown in figure (3). Figure (4), gives a simple traverse mechanism is mounted at these slots, such that the properties of the air flowing inside the test section can be measured using attached hygrometers at different values of elevation, depth and length. A simple traverse mechanism is consisting of the sliding ruler (1), which contains a circular-hole (2). The hygrometer (8) of accuracy $\pm 0.1^\circ\text{C}$ mounted through this hole is used to measure the dry bulb and wet bulb temperatures at different points inside the rectangular duct.

3.3 Calculation procedure

The test section is divided to four segments of 300 mm length. By measuring the temperature at inlet and outlet of every segment, and velocity at each run, one can evaluate the local and average Nusselt number for every value of velocity. Mass flow rate of dry air can be calculated according to the following equation

$$m_{air} = A_c \cdot u_{av} \cdot \rho_{air} \quad (13)$$

Where m_{air} , ρ_{air} , A_c and u_{av} are the mass flow rate of dry air, density of dry air at the inlet of the wind tunnel, cross sectional area of duct (200×300mm²) and average velocity of air, respectively. According to the following relations, the average heat and mass fluxes can be calculated at any segment of the cooled bottom, which lies between two successive measuring positions (along the length of test section).

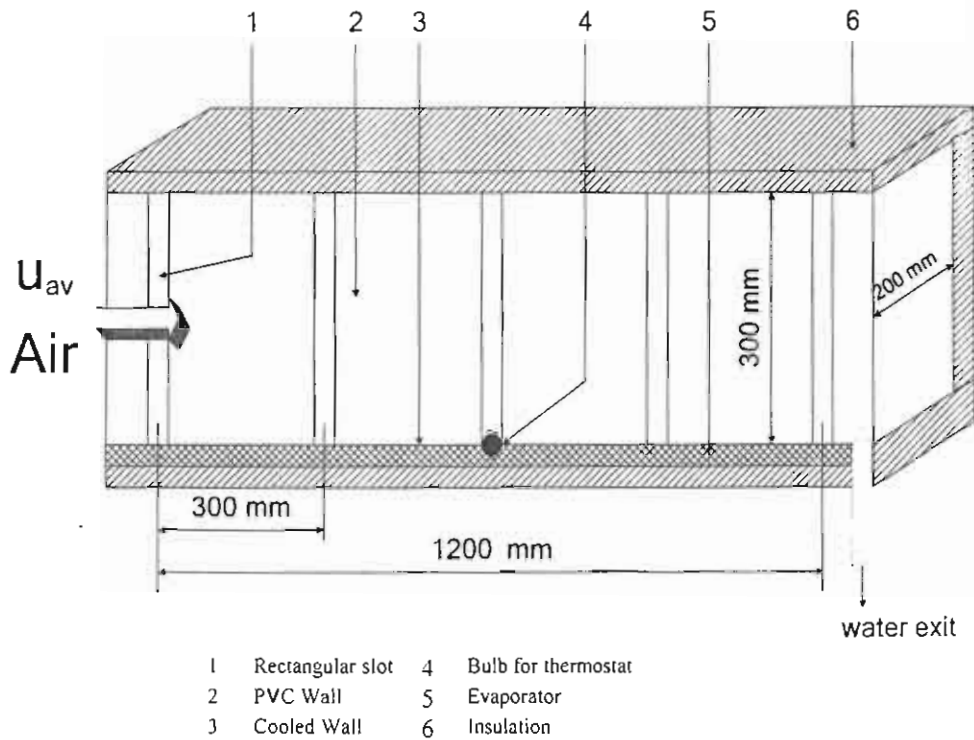


Figure (3) test section

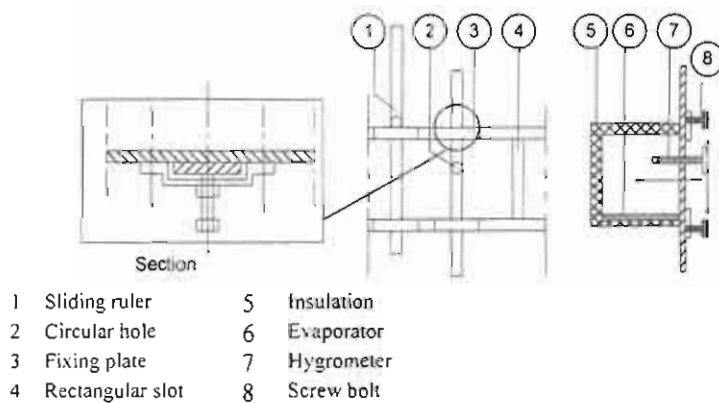


Figure (4) Simple designed traverse mechanism

$$q'' = \frac{\dot{m}_{air}}{A_s} \cdot \Delta i, \quad \dot{m}'' = \frac{\dot{m}_{air}}{A_s} \cdot \Delta w \quad (14)$$

Where q'' is heat flux and \dot{m}'' is the mass flux. A_s is the surface area of the considered segment, Δi and Δw are the difference of the enthalpy and humidity ratio between the inlet and outlet of the considered segment. The specific enthalpy i and humidity ratio w are determined

from moist air properties tables [11], knowing the average dry and wet bulb temperatures at the considered section. Accordingly, one can calculate heat and mass transfer coefficients as follows:

$$h_x = \frac{q''}{(T_\infty - T_w)}, \quad hm_x = \frac{m''}{(\rho_\infty - \rho_w)} \quad (15)$$

Where h_x and hm_x are heat transfer coefficient and mass transfer coefficient, T_∞ is dry bulb temperature for moist air far from the cooled bottom, while, T_w is cooled wall temperature, and ρ_w is density of saturated vapor at cooled wall temperature and ρ_∞ is density of vapor far from the cooled bottom.

Accordingly, one can calculate local Reynolds, Nusselt and Sherwood numbers as:

$$Re_x = \frac{u_{av} \cdot x}{\nu}, \quad Nu_x = \frac{h_x \cdot x}{k} \quad \& \quad Sh_x = \frac{hm_x \cdot x}{D} \quad (16)$$

Where ν , k and D are kinematic viscosity, thermal conductivity of dry air and mass diffusion coefficient respectively.

Then one can calculate the average Reynolds, Nusselt, and Sherwood numbers as:

$$Re_L = \frac{u_{av} L}{\nu}, \quad Nu_L = \frac{1}{L} \int_0^L Nu_x \cdot dx \quad \& \quad Sh_L = \frac{1}{L} \int_0^L Sh_x \cdot dx \quad (17)$$

Where L is total length the cooled plate.

4. Results and Discussion

In this section the obtained theoretical and experimental results are presented and discussed. Accordingly, the theoretical results including, derived profiles of dimensionless velocity, temperature and concentration in the condensation film of humid air as well as the local and average heat transfer and mass transfer coefficients are presented. In the experimental results, dry bulb and wet bulb temperatures, local and average heat transfer, mass transfer coefficients and local, average Nusselt and Sherwood numbers are depicted. Also a comparison between the present results and that of previous available works are also presented in this section.

4.1 Theoretical results

In this section the effects of the operating parameters such as Reynolds number, Prandtl and Schmidt numbers are presented.

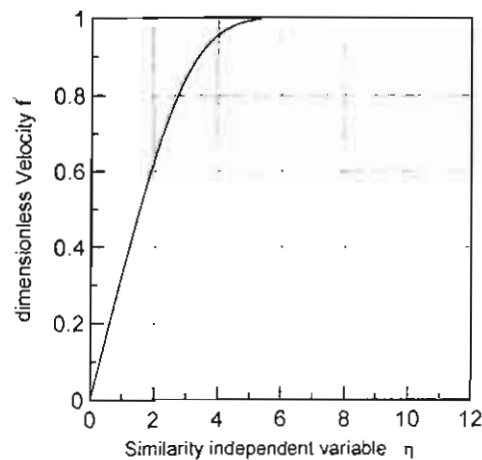


Figure (5) dimensionless velocity distribution, theoretical results

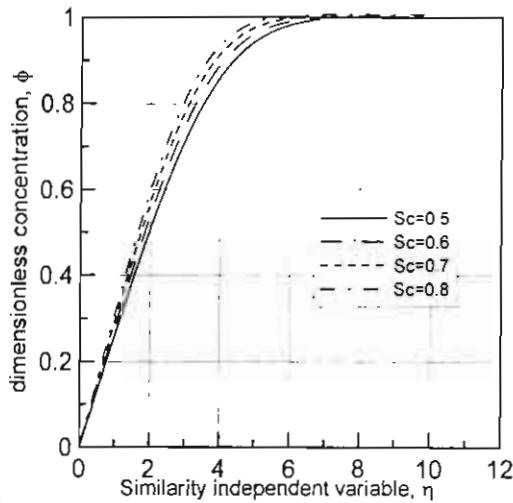


Figure (6) dimensionless concentration distribution, theoretical results

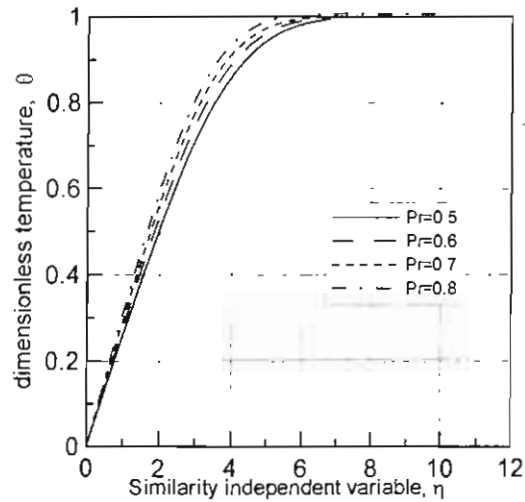


Figure (7) dimensionless temperature distribution, theoretical results

Figures (5-8) show the dimensionless velocity, temperature and concentration distribution at different values of Prandtl and Schmit numbers. In general, the velocity, temperature and concentration increase rapidly for smaller values of dimensionless independent variable η up to certain value ($\eta \approx 3$ for velocity profile), then they increase slowly, till they approach an asymptotic value of one.

As it is expected, referring to equations (8,9-a and 10), the curves of dimensionless temperature and dimensionless mass concentration versus dimensionless similarity variable (η) in case of Prandtl number and Schmidt number of 1.0 are identical to that of dimensionless velocity as shown in figure (5).

Referring to figures (6 and 7), it is clear that for higher values of Prandtl or Schmidt numbers, the temperature and concentration have higher values (for values of η up to about six). Also it is noted that for all values of Pr and Sc, temperature and concentration have an asymptotic value of one.

Figure (8) depicts the temperature distribution in case of presence of interaction between heat and mass transfer [see equation (9-b)]. In this case, the dimensionless temperature (θ) exhibits an overshoot. Which is, perhaps, due to increase of heat generated due to the condensation compared with the heat transferred by convection which in turn yields to heat concentration within the condensate film.

Figures (9) show local Nusselt number and Sherwood number against local Reynolds number at different values of Prandtl number and Schmit number, respectively.. The value of Nusselt number and Sherwood number, generally, increase with increasing Reynolds number. The effect of Pr is shown in figure (9-a). Nusselt number increases as Prandtl number increases. The behavior of Sherwood number looks like that of Nusselt number, as shown in figure (9-b). As a result of the comparison between figures (9-a and 9-c), Nusselt number is

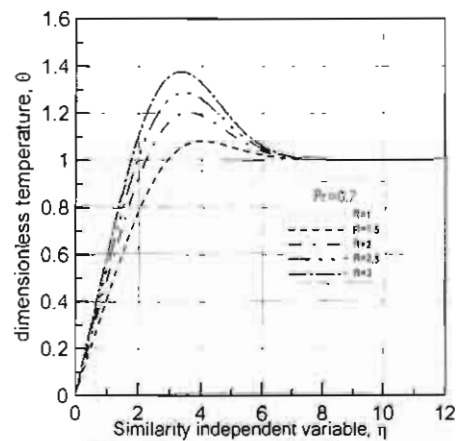


Figure (8) dimensionless temperature distribution in case of mass-heat interaction, theoretical results

higher in case of presence of interaction between heat and mass transfer for all values of

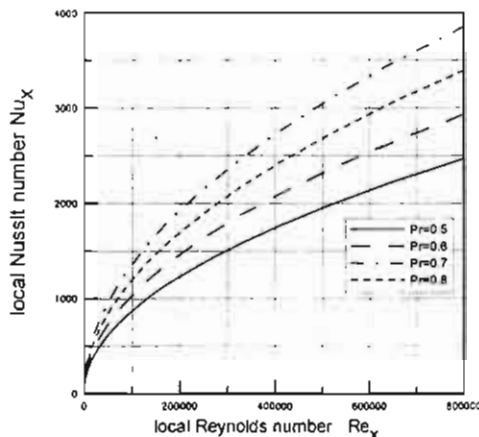


Figure (9-a) Relation between local Nusselt and Reynolds number at different values of Prandtl number, theoretical results

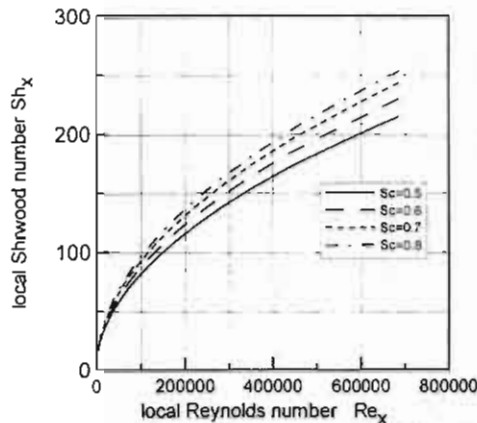


Figure (9-b) Local Sherwood number versus Reynolds number at different values of Schmidt number, theoretical results

Prandtl number.

4.2 Experimental Results

Figure(10) shows samples of temperature distribution at different dimensionless longitudinal position ($X=0$ to 1.0). From figure (10-a), the dry bulb temperature has minimum value (temperature of cooled plate) at dimensionless vertical distance $Y=0.0$ and takes an asymptotic value far from the cooled plate. The wet bulb temperature takes the same trend of that of the dry bulb temperature as shown in figure (10-b). As shown in figures(10), dry and wet bulb temperatures decrease in down stream direction.

Figures (11-a and 11-b) show the relation

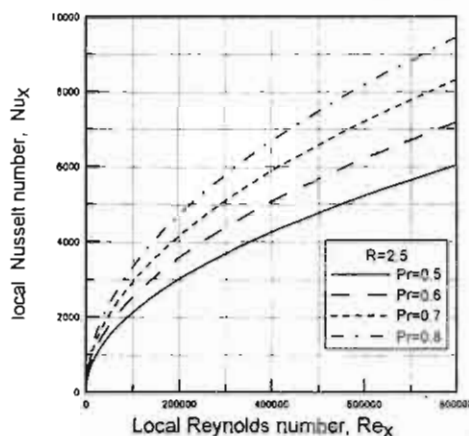


Figure (9-c) Relation between local Nusselt number and Reynolds number at different values of Prandtl number in case of mass-heat interaction, theoretical results

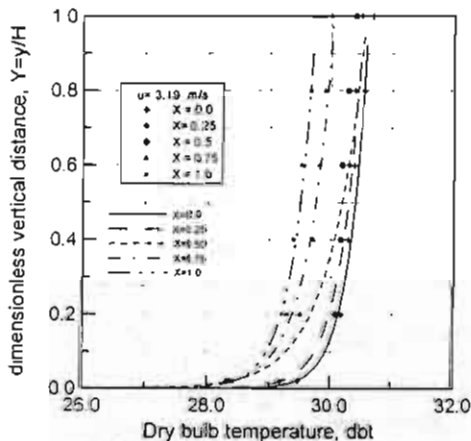


Figure (10-a) Dry bulb temperature profiles at different longitudinal dimensionless positions, at $u = 3.19$ m/s

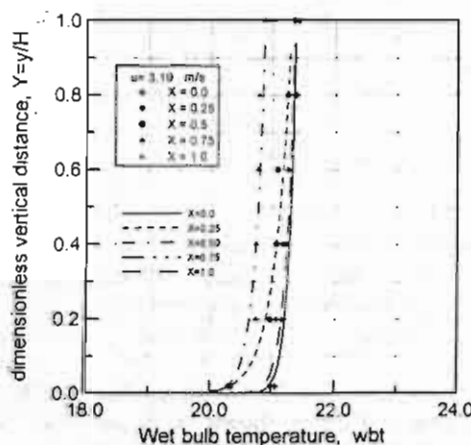


Figure (10-b) Wet bulb temperature profiles at different longitudinal dimensionless positions, at $u = 3.19$ m/s

between, local Nusselt number and local Sherwood number at different values of local Reynolds number (each four points represent the results of one case). The local Nusselt number and local Sherwood number, as well, take a minimum value at low local Reynolds number and increase with increasing local Reynolds number.

Figure (12) shows average Nusselt and Sherwood numbers against different values of Reynolds number (based on plate length equal 1.2 m). The average Nusselt and Sherwood numbers have a minimum value at the lowest value of Reynolds number and increase with increasing Reynolds number up to $Re=500,000$, there they have two peaks. Then they

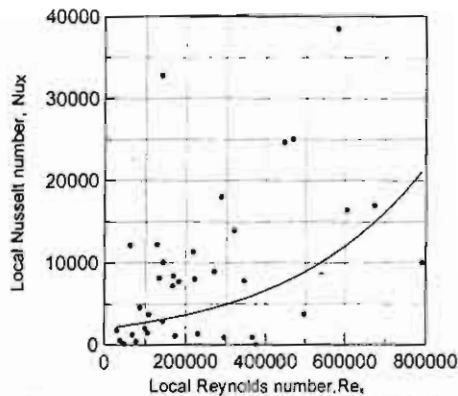


Figure (11-a) Relation between local Nusselt number for different values of local Reynolds number

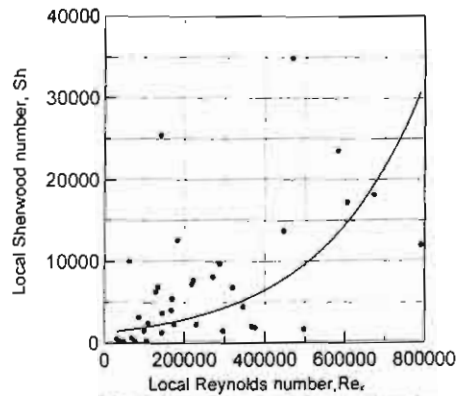


Figure (11-b) Relation between local Sherwood number at different values of local Reynolds number

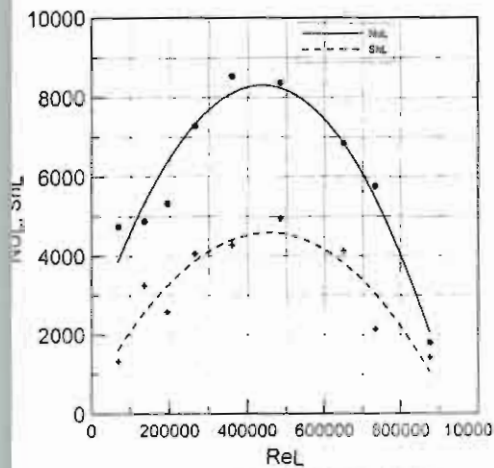


Figure (12) Relation between average Nusselt and Sherwood numbers against Reynolds number

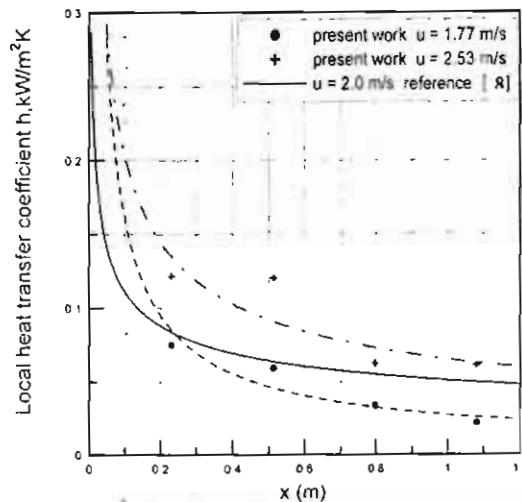


Figure (13) Comparison between local heat transfer coefficient along the plate

decrease with increasing Reynolds number, due to the migration of the water bubble with the humid airflow. Because of this migration, the rate of condensation, and in turn, rate of heat transfer is decreased.

Figure (13) shows local heat transfer coefficient along the plate of present experimental work and that after [8]. As it is clear, both are in good agreement, especially for $X > 0.2$.

Conclusion

In the present work, the condensation process of water vapor from moist air is, theoretically and experimentally, analyzed. The effects of process parameters are investigated. These parameters are presented by the following dimensionless physical quantities Prandtl, Schmidt and Reynolds numbers. Considering the theoretical proposed model, it is found that the increase of Prandtl and Schmidt numbers cause increase of Nusselt and Sherwood numbers.

According to the proposed experimental model, there is an optimum value of Reynolds number, thereafter the increase of flow velocity, and in turn, the Reynolds number cause a decrease of condensation rate, and in turn, Nusselt and Sherwood numbers. For the present operating conditions, this value of Reynolds number is found to be about 5×10^3 . The corresponding values of Nusselt and Sherwood numbers are about 9×10^3 and 4×10^3 respectively.

The following relations correlate the experimental results, where the Nusselt and Sherwood numbers are expressed as functions of Reynolds, Prandtl and Schmidt numbers:

$$Nu_x = 2.61 Re_x^{0.64} Pr^{0.34}$$

$$Sh_x = 2.12 Re_x^{0.612} Sc^{0.34}$$

The Carried out comparisons between the present and previous study exhibit a fairly good agreement.

REFERENCES

- [1] **F. Legay, Desesquelles And B. Pruunet-Foch (1985)** "Dynamic Behavior of a boundary Layer with condensation along flat plate; comparison with suction" *Int. J. Heat and Mass Transfer*, Vol. 24, No. 12, pp. 2363-2370.
- [2] **F. Legay, Desesquelles And B. Pruunet-Foch (1985)** "Heat and Mass Transfer with condensation in Laminar and turbulent boundary Layers along a flat plate" *Int. J. Heat Mass Transfer*, Vol. 29, No. 1, pp. 95-105.
- [3] **A. Matuszkiewicz and PH. Vernier (1991)** "Two-Phase Structure Of The Condensation Boundary Layer With A Non- Condensation Gas And Liquid Droplets" *Int. J. Multiphase Flow*, Vol. 17, No. 2, pp. 213-225.
- [4] **M. A. Yaghoubi, H. Kazeminejad, and A. Farshidiyanfa (1993)** "Heat and Mass Transfer With Dehumidification in Laminar Boundary Layer Flow Along a Cooled Flat Plate" *The ASME. J. Heat . Transfer*, Vol. 115, August, pp. 785-788
- [5] **Wel-Mon Yan (1995)** "Transport phenomena of developing laminar mixed convection heat and mass transfer in inclined rectangular ducts" *Int. J. Heat Mass Transfer*, Vol. 38, No. 15, pp. 2905-2914.
- [6] **Y. Sun, I. S. Gartshore and M. E. Salcudean (1995)** "An Experimental Investigation of Film Cooling Heat Transfer Coefficients Using the Mass / Heat Analogy" *ASME. J. Heat. Transfer*, Vol. 117, November, pp. 851-858.
- [7] **Kuan-Tzong Lee (1998)** "Mixed Convection Heat Transfer in Horizontal Rectangular Ducts with Wall Transpiration Effects" *Int. J. Heat Mass Transfer*, Vol. 41, No. 2, pp. 11-423.
- [8] **Hie Chan Kang, Moo Hwan Kim (1999)** "Characteristics of film condensation of supersaturated steam - air mixture on a flat plate" *Int. J. Multiphase Flow*, Vol. 25, pp. 1601 - 1618.
- [9] **Amr A. G. Akram A. M. Mohammed A. T. and Ramadan A. M. (2001)** "Effect of Cold Surface and Ambient Conditions on Water Extraction from Atmospheric Air" *12th int. M.P.E.C, Mansoura. Egypt*, Vol. 2, pp. H1-H9
- [10] **Marzouk A. Omer (2003)** "Analysis of Vapor Condensation Process from Moist Air" *M.Sc Thesis, Faculty of Engineering, Mansoura University*
- [11] **Claus Borgnakke and Richard E. Sonntag** "Table of Thermodynamic and transport Properties" *John Wiley & sons Inc 1997*.